Available online at www.sciencedirect.com
SCIENCE DIRECT®

Tectonophysics 420 (2006) 239–252

TECTONOPHYSICS

www.elsevier.com/locate/tecto

Crustal structure of mainland China from deep seismic sounding data

Songlin Li [a,1], Walter D. Mooney [b,*], Jichang Fan [a]

[a] Research Center of Exploration Geophysics, China Earthquake Administration, 104 Wenhua Road, Zhengzhou, Henan 450002, P.R. China
[b] U.S. Geological Survey, 345 Middlefield Road, MS 977, Menlo Park, CA 94025, USA

Received 19 January 2005; received in revised form 17 October 2005; accepted 4 January 2006
Available online 6 June 2006

Abstract

Since 1958, about ninety seismic refraction/wide angle reflection profiles, with a cumulative length of more than sixty thousand kilometers, have been completed in mainland China. We summarize the results in the form of (1) a new contour map of crustal thickness, (2) fourteen representative crustal seismic velocity–depth columns for various tectonic units, and, (3) a Pn velocity map. We found a north–south-trending belt with a strong lateral gradient in crustal thickness in central China. This belt divides China into an eastern region, with a crustal thickness of 30–45 km, and a western region, with a thickness of 45–75 km. The crust in these two regions has experienced different evolutionary processes, and currently lies within distinct tectonic stress fields. Our compilation finds that there is a high-velocity (7.1–7.4 km/s) layer in the lower crust of the stable Tarim basin and Ordos plateau. However, in young orogenic belts, including parts of eastern China, the Tianshan and the Tibetan plateau, this layer is often absent. One exception is southern Tibet, where the presence of a high-velocity layer is related to the northward injection of the cold Indian plate. This high-velocity layer is absent in northern Tibet. In orogenic belts, there usually is a low-velocity layer (LVL) in the crust, but in stable regions this layer seldom exists. The Pn velocities in eastern China generally range from 7.9 to 8.1 km/s and tend to be isotropic. Pn velocities in western China are more variable, ranging from 7.7 to 8.2 km/s, and may display azimuthal anisotropy.

Keywords: China; Crustal structure; Deep seismic sounding

1. Introduction

The geology of China is highly diverse. The tectonic setting ranges from the Archean core of the Sino-Korean Platform to the active continent–continent collision in the Tibet Plateau. Knowledge of the deep structure of the crust is of great importance for the study of evolutionary processes and related geodynamics. In addition, this knowledge is important for locating earthquake hypocenters, and for understanding the mechanism by which strong earthquakes are generated in China. China is a country with a high level of seismic activity, and strong earthquakes have caused great losses of people's lives and property. Therefore, it is useful to provide an updated summary of the crustal structure of China based on all available data. At the time of the previous summary of the crustal structure of China (Li and Mooney, 1998), there were 41 refraction/wide angle reflection profiles with a total length of more than thirty thousand km. Seven years later, both the profile number and the total length have approximately doubled. At the same time, data quality has also improved. We follow the convention of using the abbreviation DSS (Deep Seismic Sounding) to refer to these active source seismic profiles.

* Corresponding author. Tel.: +1 650 329 4764; fax: +1 650 329 5163.
E-mail address: mooney@usgs.gov (W.D. Mooney).
[1] Tel.: +86 371 393 4547; fax: +86 371 393 7341.

0040-1951/$ - see front matter © 2006 Published by Elsevier B.V.
doi:10.1016/j.tecto.2006.01.026

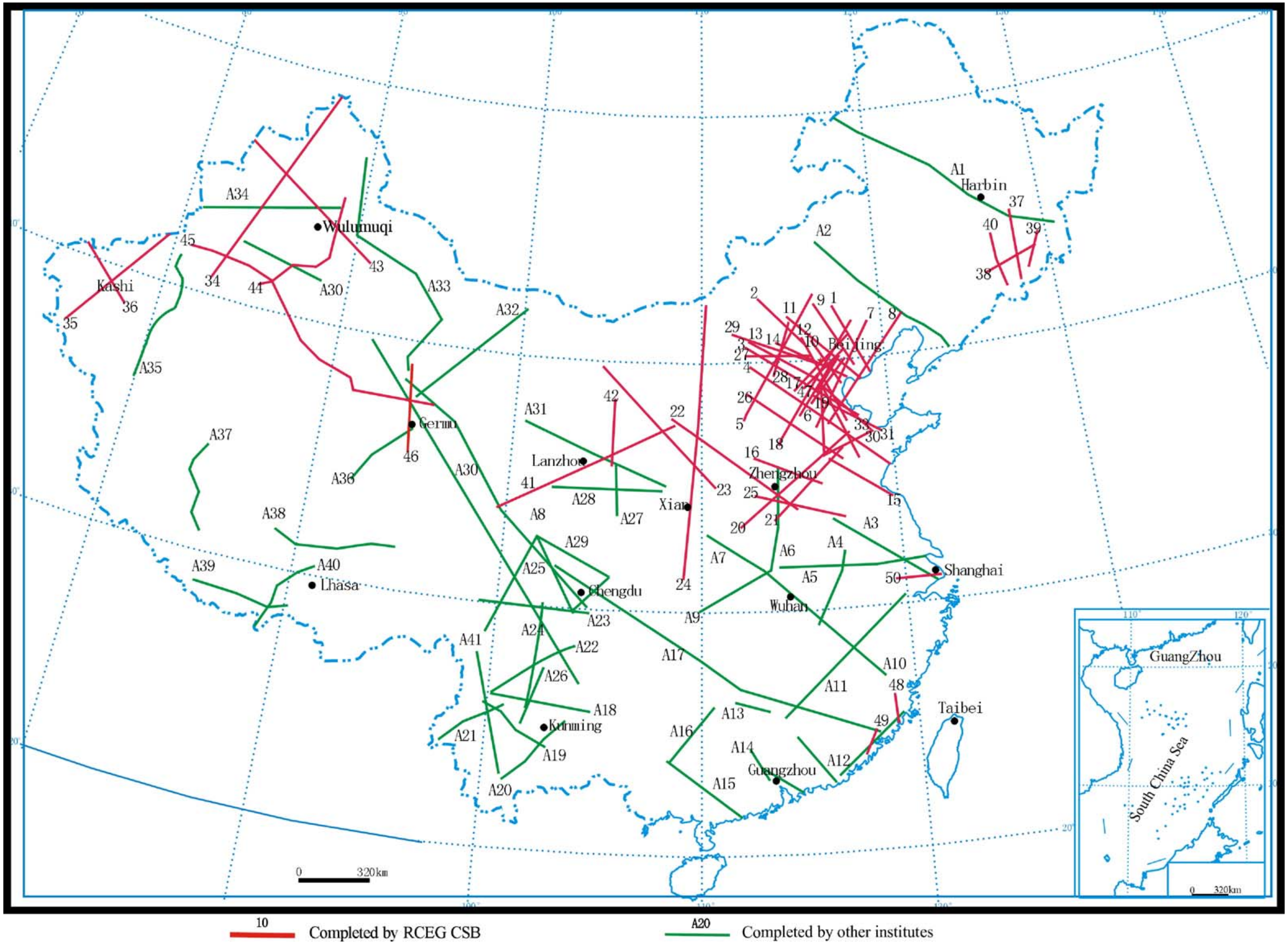

Fig. 1. Position map of refraction/wide angle reflection profiles in mainland China. Red lines represent profiles completed by RCEG, CEA (Research Center of Exploration Geophysics, China Earthquake Administration). The number of each profile is written near it and is the same as that listed in Table 1. Green lines are profiles by other institutions. Their profile numbers are represented by a capital letter "A" and a number and are the same as those listed in Table 2.

2. Profile location, data processing and interpretation

Some 90 DSS profiles have been recorded in mainland China, among which 49 were completed by the Research Center of Exploration Geophysics (RCEG), China Earthquake Administration (CEA, previously known as the China Seismological Bureau or CSB), the country's main DSS institute. Fig. 1 shows locations of these profiles. While the red lines

Table 1
Information of refraction/wide angle reflection profiles completed by RCEG (Research Center of Exploration Geophysics, China Earthquake Administration, 2004)

No.	Symbol	Name	Length (km)	Azimuth	Shots	Observing time
1	I	Changli-Chengde-Dalainuoer	364.0		4	1984
2	II	Beijing-Zhangjiakou-Huade	300.0	318°46′	4	1984
3	III	Haixing-Yangyuan-Fengzheng	579.0	305°30′	9	1980
4	IV	Zhucheng-Dingxian-Tuoketuo	774.2		7	1983, 1984
5	V	Taiyuan–Xuanhua	650.0		6	1983
6	VI	Renxian–Hejian–Wuqing	431.0	50°20′	10	1980
7	VII	Changzhou-Tianjin-KaLaqinzuoyi	510.0		8	1982, 1984
8	VIII	Dezhou-Qinhuangdao	587.0		9	1983
9	H-01	Baigezhuang-FengNing-Zhenglanqi	407.0		7	1979
10	H-02	Tanggu-Sanhe–Miyun	220.0		4	1979
11	H-03	Nanbao-Chicheng-Kangbao	493.0	314°2		1981
12	H-04	Yanshan-Daxin-Yanqing	476.0	333°05′8		1979
13	H-05	Leting-Zhangjiakou	440.0	295°15′	10	1976, 1981
14	H-06	Ninghe-Beijing–Zhuolu			10	1978
15	H-07	Lianyungang-Lingyi-Sishui	328.0		15	1980
16	H-08	Hezhe-Lingzhou-Changzhi	304.0	294°50′	8	1981
17	H-10	Anguo-Yongqin-Zhonghua	350.0	50°36′	9	1977, 1981
18	H-11	Shijiazhuang–KaLaqinqi	746.0	35°	10	1982
19	H-12	Hejian-Wuqing	168.0	35°04′	2	1981
20	H-13	Zhengzhou-Jinan	600.0	58°30′	5	1984
21	H-14	Xiangcheng-Hezhe-Zhangqiu	488.0	59°05′	2	1983
22	H-15-1	Zhengzhou-LingFen-Jingbian	633.0	309°	5	1985
23	H-15-2	Zhengzhou-Yinchuan (west)	680.0	312°	6	1986
24	H-16	Xi'an–Yan'an-Baotou-Baiyunebo	1120.0		8	1987
25	H-18	Lingbi-Zhengzhou	501.8		9	1989
26	H-19	Taian-Longyao-Xinxian	480.0		6	1992
27	H-20	Beijing-Huailai–Fengzhen	342.0		7	1993
28	H-21	Fanzhi-Huailai-Taipushiqi	302.0		5	1993
29	H-21	Wenan-Weixian-Chayouzhongqi	420.0		6	1994
30	L1	Qihe-Zhangqiu-Shouguang	240.0	75°	3	1993
31	L2	Shouguang-Zhanhua-Wenan	291.0	315°	3	1993
32	L3	Wenan-Dezhou-Qihe	290.0	3°	4	1993
33	L4	Yiyuan-Lelin-Dacheng	315.0	345°	6	1993
34	KDB	Kuche-Dushanzhi-Buerjin	950.0		9	1997
35	JA1	TashiKuergan-Jiashi-Arheqi	533.0		5	1998
36	JA2	Shache-Artushi-Yuoyun	295.0		4	1998
37	CHBSH-L1	Changbai-Dunhua	270.0		4	1998
38	CHBSH-L2	Jingyu-Zhaoyangchuan	250.0		3	1998
39	CHBSH-L3	Guangping-Zhaoyangchuan	120.0		2	1998
40	CHBSH-L4	Badaogou-Huadian	180.0		3	1998
41	MLJ	Maqin-Lanzhou-Jingbian	941.6		9	1998
42	XHZH	Xiji-Haiyuan-Zhongwei	248.0		3	1999
43	QKM	Qitai-Kelamayi-Erming	620.0	300°	8	2000
44	KTJ	Kuerle-Tuokexun-Jimsaer	600.0		5	2000
45	DRB	Dachaidan-Ruoqiang-Baicheng	1292.4		10	2000
46	GDH	Germu-Dachaidan-Huahaizhi	353.6		3	2000
47	XXK	Anxing-Xianghe-Kuancheng	320.0		4	2003
48	JSHNH	Jiangtian-Shangganyu-Hongwei	80.0		16	2003
49	ZHT	Zhangpu-Tongan	160.0	41°	9	2003

Table 2
Profiles completed by other units and corresponding references

A1 Manzhouli–Suifenhe geoscience section, Yang et al. (1994)
A2 Luyang–Haicheng–Donggou deep seismic sounding profile, Lu et al. (1988)
A3 Fengxian–Lingbi (HQ–13) geoscience section, Chen et al. (1993)
A4 Zhuangmu–Zhanggongdu profile, Wang et al. (1997)
A5 Shuixian–Maanshan profile, Zheng et al. (1989)
A6 Shuixian–Anyang profile, Hu et al. (1986)
A7 Shuixian–Xiyang profile, Ding et al. (1987)
A8 Aljin–Longmenshan geoscience section, Wang et al. (2004)
A9 Jiajiawan–Shayuan profile, Chen et al. (1988)
A10 Ningde–Yongping–Xinyang profile, United Observing Group, State Seismological Bureau (1988)
A11 Hangzhou–Yongping–Ganzhou profile
A12 Fuzhou–Yongping–Shantou profile, Liao (1988)
A13 Qiziqiao–Lingxian profile, Li et al. (1988)
A14 (We do not know the name of this profile.)
A15Yangjiang–Liuzhou profile, Liuzhou Explosion Observing Group, Guangxi (1988)
A16 Liuzhou–Quanzhou profile, Liuzhou Explosion Observing Group, Guangxi (1988)
A17 Heishui–Shaoyang–Quanzhou profile, Cui et al. (1996).
A18 Lijiang–Zhehai profile, Xong et al. (1986).
A19 Er yuan–Jiangchuan profile, Hu et al. (1988)
A20 Simao–Malong profile, Kan et al. (1988)
A21 Zhefang–Bingchuan profile, Hu et al. (1988)
A22 Lijiang–Xinshizhen profile, Cui et al. (1987).
A23 Zhubalong–Zizhong profile, Wang et al. (2003)
A24 Lijiang–Panzhihua–Zhehai profile, Xun (1993)
A25 Tangke–Bengzilan profile, Wang et al. (2003).
A26 Xichang–Muding profile, Yi et al. (1992).
A27 Chengxian–Xiji profile, Li (1991)
A28 Lingtai–Amuquhu profile, Min (1991)
A29 Tangke–Pujiang–Langzhong profile, Chen (1988)
A30 Tianshan–Luobubo–Dongchuan profile, Song et al. (1988)
A31 Menyuan–Pingliang–Weinan profile, Zhang (1985)
A32 Golmud–Ejinaqi Geoscience section, Cui (1995)
A33 Altay–Hami–Akesai profile, Wang et al. (2003)
A34 Urumqi–Zhaosu profile, "Accomplishments of Deep Geophysical Prospecting" Compiling Group, State Seismological Bureau
A35 Xinjiang Geoscience section (Quanshuigou–Dushanzi), Li et al. (2001)
A36 Tuotuohe–Golmud profile, Lu et al. (1990)
A37 Cuoqin–Gaize–Sangehu profile, Pan et al. (1998)
A38 Selincuo–Pengcuo–Naqu–Suoxian profile, Teng et al. (1985)
A39 Peigucuo–Dingjie–Pumoyongcuo profile, Teng et al. (1983)
A40 Dangxong–Yadong profile, Institute of Geophysics, Chinese Academy of Science (1981)
A41 Simao–Zhongdian profile, Hu et al. (1986).

A1 Yang, B.J., Liu, C., Liang, T. Ch. et al., 1994. Manzhouli–Suifenhe geoscience section, edited in chief by Jing, X., Yang, B.J., Study on Geophysical and Deep Structure Features of Manzhouli–Suifenhe Geoscience Section, in China, Beijing: Seismological Press, 75–85.
A2 Lu, Z.X., Zhang, G.Ch., Li, J.Zh. et al., 1998, An explosion-seismology study on structure of crustal and upper mantle in South Liaoning province, In: Developments in the Research of Deep Structures of China's Continent, Beijing: Geological Publishing House 114–128.

Table 2 (*continued*)

A3 Chen, H.Sh. et al. (chief editor), 1994, An Instruction Book of Lingbi–Fengxian (HQ–13) Geoscience Section, Beijing: Geological Publishing House, 21–43.
A4 Wang, Ch.Y., Zhang, X.K., Chen, B.Y. et al., 1997, Study on crustal structures in Dabie orogenic belt, Science in China (Series D), 27: 221–226.
A5 Zheng, Y., Teng, J.W., 1989, Crustal and upper mantle structures of Suixian–Maanshan region and some features of structures in the southern part of Tanlu tectonic belt, Chinese J Geophys, 32: 648–659.
A6 Hu, H.X., Chen, X.B., Zhang, B.X. et al., 1986, Interpretation of deep seismic sounding data along Shuixian–Anyang profile in central China, Acta Seismologica Sinica, 8: 37–49.
A7 Ding, W.Y., Cao, J.M., Huang, Ch.L. et al., 1987, Preliminary research of crustal structures along Suixian–Xi'an profile, Chinese J Geophys, 30: 31–38.
A8 Wang, Y.X., Han, G.H., Yuan, X.Ch. et al., 2004, The velocity structure of crust along Aljin–Longmenshan geoscience section, Study on the Deep Structure and Dynamics of Earth in Chinese Continent, Beijing: Scientific Press, 134–152.
A9 Chen, B.Y., Gao, W.X., 1988, The deep structure of crustal and upper mantle along Jiajiawan–Shawan profile In: Developments in the Research of Deep Structures of China's Continent, Beijing: Geological Publishing House, 154–168.
A10 Yongping Explosion Observing Group, SSB, 1988, The preliminary research of Yongping explosion and deep structure in southeast China, In: Department of Scientific Programming and Earthquake Monitoring ed Developments in the Research of Deep Structures of China's Continent, Beijing: Geological Publishing House, 140–153.
A11 Yongping Explosion Observing Group, SSB, 1988, The preliminary research of Yongping explosion and deep structure in southeast China, In: Department of Scientific Programming and Earthquake Monitoring ed Developments in the Research of Deep Structures of China's Continent, Beijing: Geological Publishing House, 140–153.
A12 Liao, Q.L., Wang, Zh.M., Wang, P.L., An explosion-seismology study on crustal structure in Fuzhou–Quanzhou–Shantou areas
A13 Li, Y.F., Xu, Zh.Ch. et al., 1988, Seismological observation of Qiziqiao explosion, In: Developments in the Research of Deep Structures of China's Continent, Beijing: Geological Publishing House, 180–191.
A14 (We do not know the reference about this profile.)
A15 Liuzhou Explosion Research Group, 1988, Observation of Liuzhou explosion and the crustal structure in eastern Guangxi, In: Developments in the Research of Deep Structures of China's Continent, Beijing: Geological Publishing House, 246–252.
A16 Liuzhou Explosion Research Group, 1988, Observation of Liuzhou explosion and crustal structure in eastern Guangxi, In: Developments in the Research of Deep Structures of China's Continent, Beijing: Geological Publishing House, 246–252.
A17 562 Comprehensive Brigade, Chinese Academy of Geology Sciences, 1988, An explosion-seismology study report of Heishui–Shaoyang (the western part of Heishui–Quanzhou geoscience section). The investigative report of deep geophysics along Heishui–Shaoyang profile in South China.
A18 Xong, Sh.B., Teng, J.W., Yi, Zh.X. et al., 1986, An explosion-seismology study on crust–mantle structures in southern part of Panxi tectonic belt, Chinese J Geophys 29(3), 235–244.

Table 2 (*continued*)

A19 Hu, H.X., Lu, H.X. and Wang, Ch.Y. et al., 1988, An explosion-seismology study on crustal structures in Dianxi area, In: Developments in the Research of Deep Structures of China's Continent, Beijing: Geological Publishing House, 253–266.
A20 Kan, R.G., Hu, H.X., Zheng, R.Sh., 1988, The crustal structure and evolution from seismic refraction profiles in Yunnan province, China, In: Developments in the Research of Deep Structures of China's Continent, Beijing: Geological Publishing House, 253–266.
A21 Hu, H.X., Lu, H.X., Wang, C.Y. et al., 1988, An explosion-seismology study on crustal structures in Dianxi area, In: Developments in the Research of Deep Structures of China's Continent, Beijing: Geological Publishing House, 253–266.
A22 Cui, Z.Zh., Lu, D.Y., Chen, J.P. et al., 1987, The deep structure and tectonic of the earth's crust in Panxi area, Chinese J Geophys, 30(6), 566–580.
A23 Wang, Ch.Y., Wu J.P., Lou, H. et al, 2003, The P wave velocity structure of crust in West Sichuan and East Tibet areas, Science in China (Series D), 33, supplement, 181–189.
A24 Xiong, Sh.B., Zheng, Y., Yin, Zh.X. et al., 1993, 2-D crustal structure and its structural meanings along Lijiang–Panzihua–Zehai zone, Chinese J Geophys 36: 434–444.
A25 Wang, Ch.Y.,Han, WB.,Wu, J.P. et al., 2003, The velocity structure of crust in Songpan–Ganzi orogenic belts, Acta Seismologica Sinica, 25(3), 229–241.
A26 Yi, Zh.X., Xong, Sh.B., 1992, The explosion-seismology study on 2-D crustal structure in Xichang–Dukou–Muding zones, Chinese J Geophys, 35(4), 451–458.
A27 Li, Q.H., Guo, J.K., Zhou, M.D. et al., 1991, Crustal velocity structure along Chengxian–Xiji profile, Northwest China Earthquake Sciences, 13, supplement, 37–43.
A28 Min, X.Y., Zhou, M.D., Guo, J.K. et al., 1991, Crustal velocity structure along Lingtai–Amquhu profile, Northwest China Earthquake Sciences, 13, supplement, 29–36.
A29 Chen, X.B., Wu, Y.J., Du, P.Sh. et al., 1988, Crustal velocity structure at two sides of Longmenshan tectonic belt, In: Department of Scientific Programming and Earthquake Monitoring ed Developments in the Research of Deep Structures of China's Continent, Beijing: Geological Publishing House, 97–113.
A30 8301 Project Cooperation Group, 1988, Velocity structure of crust and upper mantle at the east margin of Tarim Basin and the east part of Qinghai–Tibet plateau, In: Department of Scientific Programming and Earthquake Monitoring ed Developments in the Research of Deep Structures of China's Continent, Beijing: Geological Publishing House 89–96.
A31 Zhang, Sh.Q., Wu, L.J., Guo, J.M., Chen, X.B., 1985, Interpretation of DSS data along Menyuan–Pingliang–Weinan profile in the west part of China, Chinese J Geophys, 28: 349–361.
A32 Cui, Z.Zh., Li, Q.Sh., Wu, Ch.D. et al., 1995, Crustal structure and deep tectonic along Golmud–Ejinaqi geoscience section, Chinese J Geophys, 38, (Supplement II): 15–28.
A33 Wang, Y.X., Mooney, W. D. et al., 2003, The crustal structure from the Altai Mountains to the Altyn Tagh fault, northwest China, J. G. R. 108 (B6), 7–16.
A34 "Deep Geophysical Accomplishments" Compiling Group, SSB, 1986, The geophysical accomplishments of crust and upper mantle in China, Beijing: Seismological Press, 243–244.
A35 Li, Q.Sh., Lu, D.Y., Gao, R. et al., 2001, Comprehensive research of deep seismic sounding geoscience section (Quanshuigou–Dushanzi) in Xinjiang, Journal of Earth Sciences, 22 (6): 534–540.
A36 Lu, D.Y., Wang, X.J., 1990, Crustal structure and deep process at Tuotuohe–Golmud region in the north part of Qinghai–Tibet Plateau, Journal of Chinese Academy of Geology Sciences, No. 21, 227–238.
A37 Pan, Y.Sh., Kong, X.R., 1998, Evolution and dynamics of lithosphere structure in Qinghai–Tibet Plateau, Guangdong Press of Science and Technology, 3–17.
A38 Teng, J.W., Yin, Zh.X., Xong, Sh.B., 1985, Crustal structure and velocity distribution along Selincuo–Pengcuo–Naqu–Suoxian zones in the north part of Tibet Plateau, Chinese J Geophys, 28, (Supplement I): 28–42.
A39 Teng, J.W., Xong, Sh.B., Yin, Zh.X. et al., 1983, Velocity distribution features and the structural model of crust in the north part of Himalayan area, Chinese J Geophys, 26: 525–540.
A40 Institute of Geophysics, Chinese Academy of Sciences, 1981, An explosion-geology study on structure and velocity distribution of crust and upper mantle along Dangxong–Yadong zones in Qinghai–Tibet Plateau, Chinese J Geophys, 24: 155–170.
A41 Hu, H.X., Lu, H.X., Wang, Ch.Y., et al., 1986 An explosion-seismology study on crustal structure in Dianxi region, Chinese J Geophys, 29(2), 133–144.

show profiles conducted by RCEG, the green lines indicate profiles by other institutes. The total length of these 90 profiles is about sixty thousand km, twenty-five thousand of which were completed by the RCEG. Information related to each profile is listed in Tables 1 and 2.

Fig. 2 shows a simplified version of the geological map of China. From Figs. 1 and 2, we can see that almost every geological unit has been profiled with DSS. However, the geographic coverage of the DSS profiles is not uniform, and tends to be more concentrated in northeastern China, especially in the Beijing–Tianjin–Tangshan Region. In recent years, several of the profiles have been completed in Xinjiang Province. As a result, northwestern China has been relatively well investigated. On the Tibetan plateau, some DSS profiling has been completed in the north-central, northeastern, and south-central parts. However, due to the difficulty of working conditions on the plateau, seismic profiles are sparse, especially in the west.

Various data processing techniques, such as band-pass filtering and seismic energy plots, have been used to enhance data quality. During the data modeling phase, relations governing the reversal and overlapping of travel-time curves were all considered to constrain phase correlation and picking (Giese et al., 1976). Travel-time inversion is the main method used to calculate 1-D and 2-D velocity models (Zelt and Smith, 1992), and with the further calculation of seismic amplitudes, important model constraints are provided (Mooney, 1989). No matter which inversion

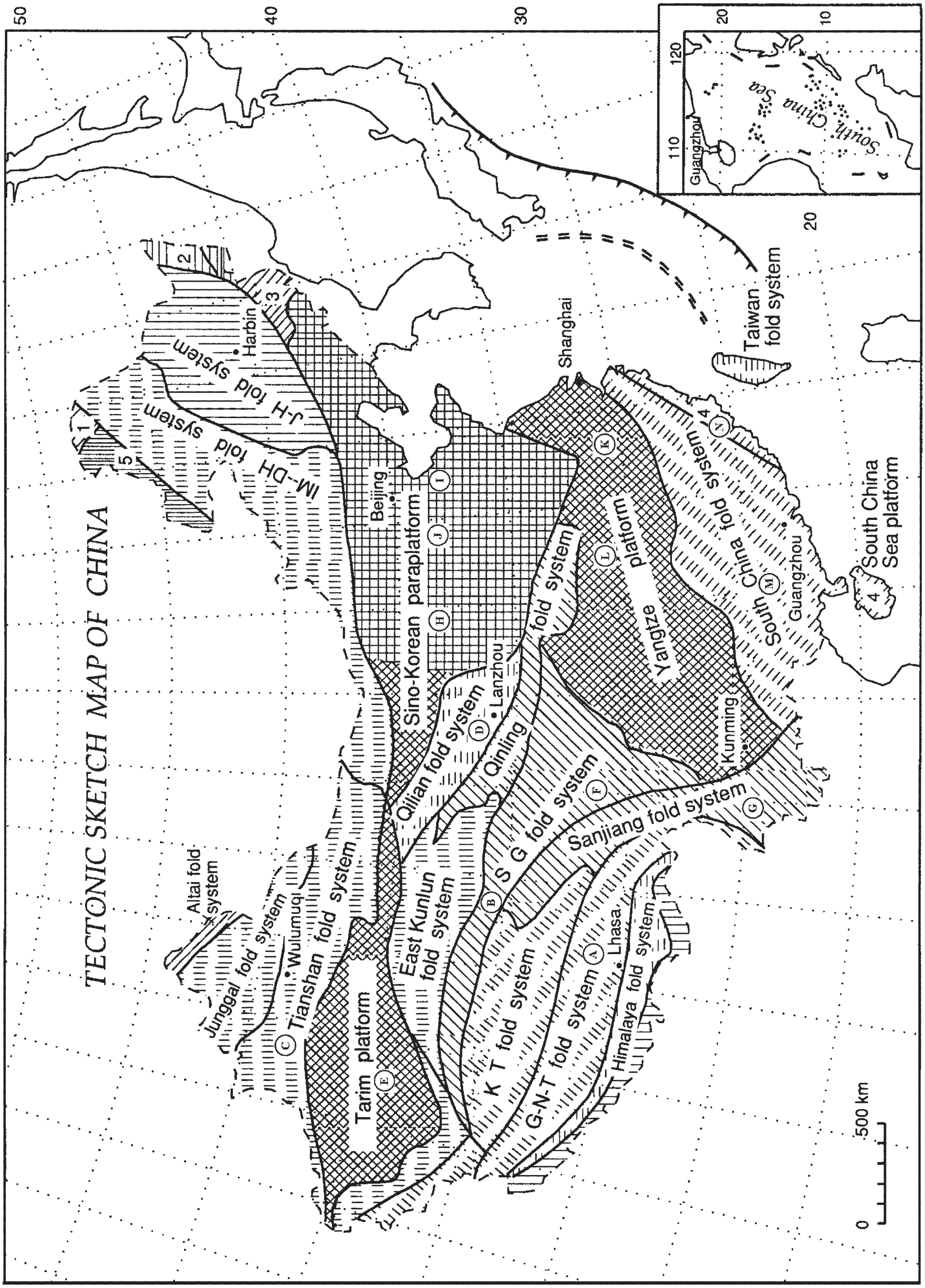
TECTONIC SKETCH MAP OF CHINA
Altai fold system
Junggal fold system
Wulumuqi
Tianshan fold system
Tarim platform
East Kunlun fold system
Qilian fold system
Qinling
Lanzhou
Sino-Korean paraplatform
Beijing
Harbin
J-H fold system
IM-DH fold system
S G fold system
K T fold system
G-N-T fold system
Lhasa
Himalaya fold system
Sanjiang fold system
Kunming
Yangtze platform
fold system
South China fold system
Guangzhou
South China Sea platform
Shanghai
Taiwan fold system
South China Sea
Guangzhou
0
500 km

method is used, it is most important to set up a reasonable initial model. Fig. 3 shows an example of the data processing.

Model resolution is closely related to both data quality, and the physical laws governing wave propagation (Mooney et al., 2002). Data quality depends on both the signal-to-noise ratio and the observational system (the number of sources and receivers and their relative spacing). Usually there are more seismic rays in the upper layers, thus allowing the upper layers to be resolved with greater accuracy. Meanwhile, the physical laws governing wave propagation limit the resolution of the profiles. Due to seismic attenuation, signals penetrating deeper will contain relatively low frequencies, thus having a lower resolution. This factor makes obtaining high resolution for the deeper layers of the crust very difficult. In addition, the methods used in data processing affect model resolution (Mooney, 1989). In the determination of an initial model from seismic refraction data, apparent seismic velocities are directly measured, while the depths of refracting horizons are successively calculated from the uppermost layer to the deepest layer. Thus, seismic velocities can usually be determined more accurately than depths. Due to these constraints, seismic velocities and interface depths are accurate to about 3% and 5%, respectively.

3. Crustal thickness

Several contour maps of the crustal thickness of China have been published within the last several years (Ma, 1989; Yuan, 1996; Li and Mooney, 1998). In view of the accumulation of new data obtained in recent years, we have created a new, more accurate map of crustal thickness with greater resolution of detail (Fig. 4). It is generally observed that the crust thickens from east to west. The crust is only 28–30 km thick along the east coast. Beneath the Tibetan plateau, it reaches a thickness of at least 74 km, the maximum value measured in the world from DSS data.

There is a north–south-trending belt, at 103–105° east longitude, with a strong lateral gradient in crustal thickness in central China. This belt coincides with the north–south seismic belt, and the associated linear Bouguer gravity anomaly (Ma, 1989). This north–south belt divides China into an eastern portion with a crustal thickness of 30–46 km, and a western portion with a thickness of 46–74 km. In western China, the crustal thickness isolines trend nearly west–east, while in eastern China they trend in the NNE direction. These observations are consistent with the findings of Li and Mooney (1998).

A new observation is the apparent relationship between crustal thickness and tectonic setting. Within depressions and basins, the crust appears thinner than in adjacent regions. Examples include: the Tarim basin, Junggar basin and Qaidam basin in western China, and the Ordos Platform, Sichuan basin, Song-Liao basin and Jiang-Han basin in eastern China. By contrast, in topographically uplifted areas, such as the Tibetan plateau and the Tianshan in the west, and the Taihang mountains and Daxingan Ling mountains in the east, the crust is thicker than in its surroundings. These relationships were only hinted at in previous studies.

4. Crustal structure and evolution

Fig. 5 shows fourteen representative crustal velocity columns that provide important insights into the evolution of the crust. The location for each column is shown in Fig. 2. The above-mentioned differences in crustal thicknesses between the two portions of China are evident in these crustal columns. In western China, the crust is normally thicker than 46 km, while in eastern China it is usually thinner than 36 km. We infer that these major differences reflect the variation in the geological evolution of these two regions, as expressed today by the distinct tectonic stress field.

While western China is mainly affected by the collision between the Indian and Eurasian Plates in the NS direction (Patriat and Achache, 1984; Dewey et al., 1989; Molnar et al., 1993), eastern China has a far more complex tectonic history. Eastern China has not only been affected by the compression between the Pacific and Eurasian Plates in the EW direction (Ma, 1989; Ding, 1991), but also by widespread rifting, Cenozoic volcanism (Liu et al., 2004), and the clockwise rotation of the South China Block throughout the Mesozoic (Meng et al., 2005). These recent and important processes dominate the crustal evolution and stress field of the east. Since the tectonic processes in western

Fig. 2. Tectonic map of China (after Huang et al., 1980). Different tectonic regimes are distinguished by patterns (diagonal lines, dashed lines, etc). Abbreviations are: IM–DH = Inner Mongolia–Da Hinganling fold system; J–H = Jilin–Heilongjiang fold system; S–G = Songpan–Ganzi fold system; K–T = Karakoram–Tanggula fold system; G–N–T = Gangdise–Nyainqentanglha fold system. Numbers represent smaller tectonic provinces and are as follows: 1 = North Ergum fold system; 2 = North Yanbian fold system; 3 = South Yanbian fold system; 4 = additional regions of the South China fold system; 5 = South Ergum fold system. Circled letters represent positions corresponding to velocity columns in Fig. 5.

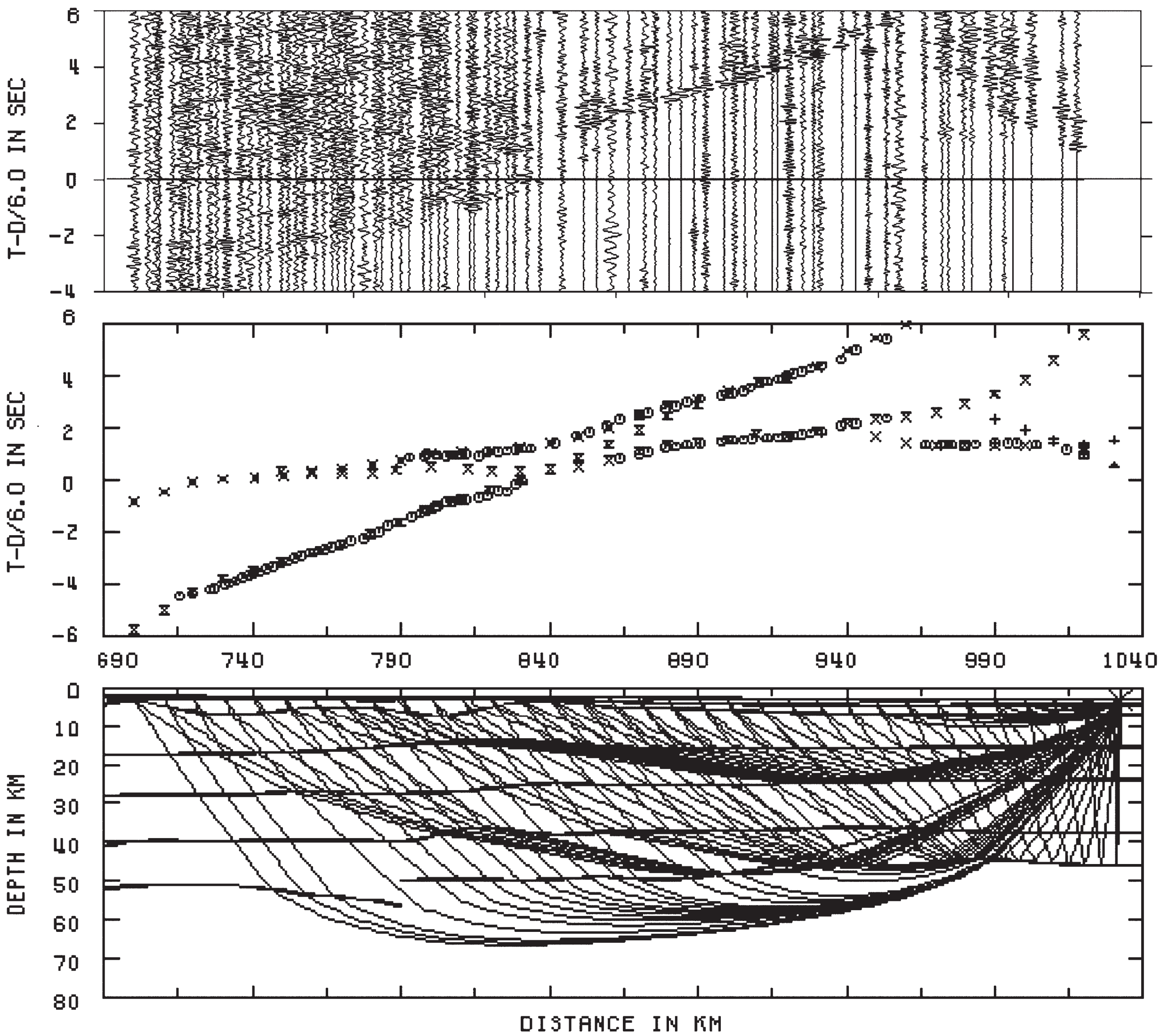

Fig. 3. Record section of Profile 973 from Shot Point 1032 (upper), its ray-tracing diagram (bottom) and travel-time curves (middle). The ray-tracing diagram is of Pg, PMP and Pn waves for the final 2-D model. The lower part shows the comparison between observed and calculated travel-times. Circles represent calculated travel-times, while signs "+" and "x" represent observed data.

China are much more active than those in the east, the crust of the western portion is strongly compressed in NS direction and has become quite thick. In contrast, the crust of eastern China has been extended and become thinner (Hsu et al., 1990; Zhao and Windley, 1990; Filatova, 2004).

As shown in Fig. 5, there exists a high-velocity (7.1–7.4 km/s) layer in the lower crust beneath three stable regions of western China. This layer is just above the Moho and consists of metamorphic mafic rocks (Christensen and Mooney, 1995) beneath the Tarim basin, the Ordos block, and North China. In contrast, this layer is generally absent beneath large portions of eastern China and young orogenic belts. One exception is found beneath the southern Tibetan plateau, where the high-velocity layer is present due to the northward injection of the cold Indian Plate (Zhao and Morgan, 1987; Zhao et al., 1993; Nelson et al., 1996). However, the high-velocity layer is absent beneath the northern Tibetan plateau. One possibility is that it has delaminated and sunk into the upper mantle. Liang et al. (2004) propose a delamination model for the Tian Shan and Gao et al. (1998) suggest that the lower crust and subcrustal lithosphere have delaminated in parts of eastern China that were subjected to Cenozoic extension.

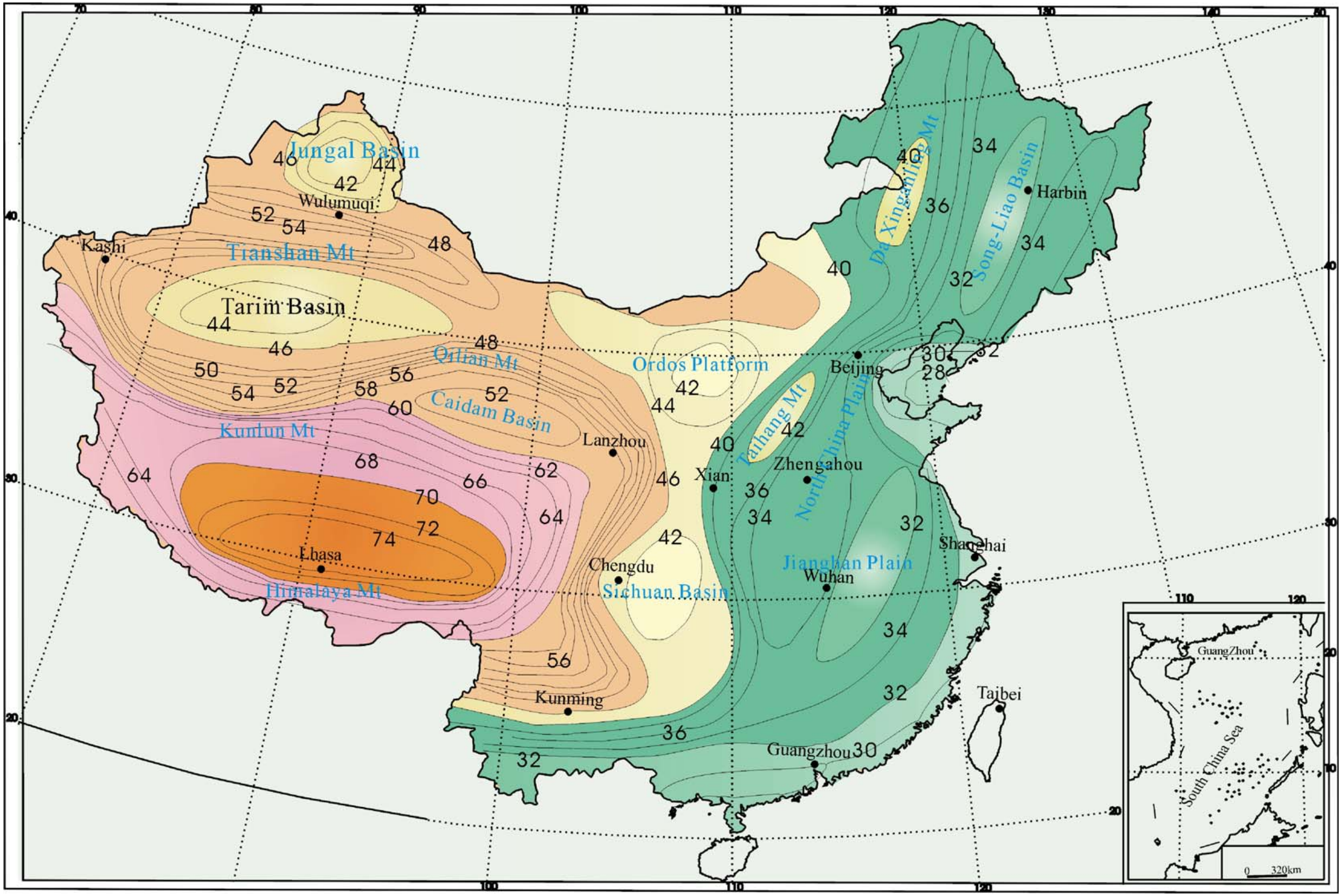

Fig. 4. Contour map of crustal thickness obtained from DSS data (Fig. 1). Contour interval is 2 km. Crustal thickness ranges from 28 to 46 km in eastern China, and from 42 to 74 in western China. The margins of the Tibetan plateau are marked by a steep gradient in crustal thickness.

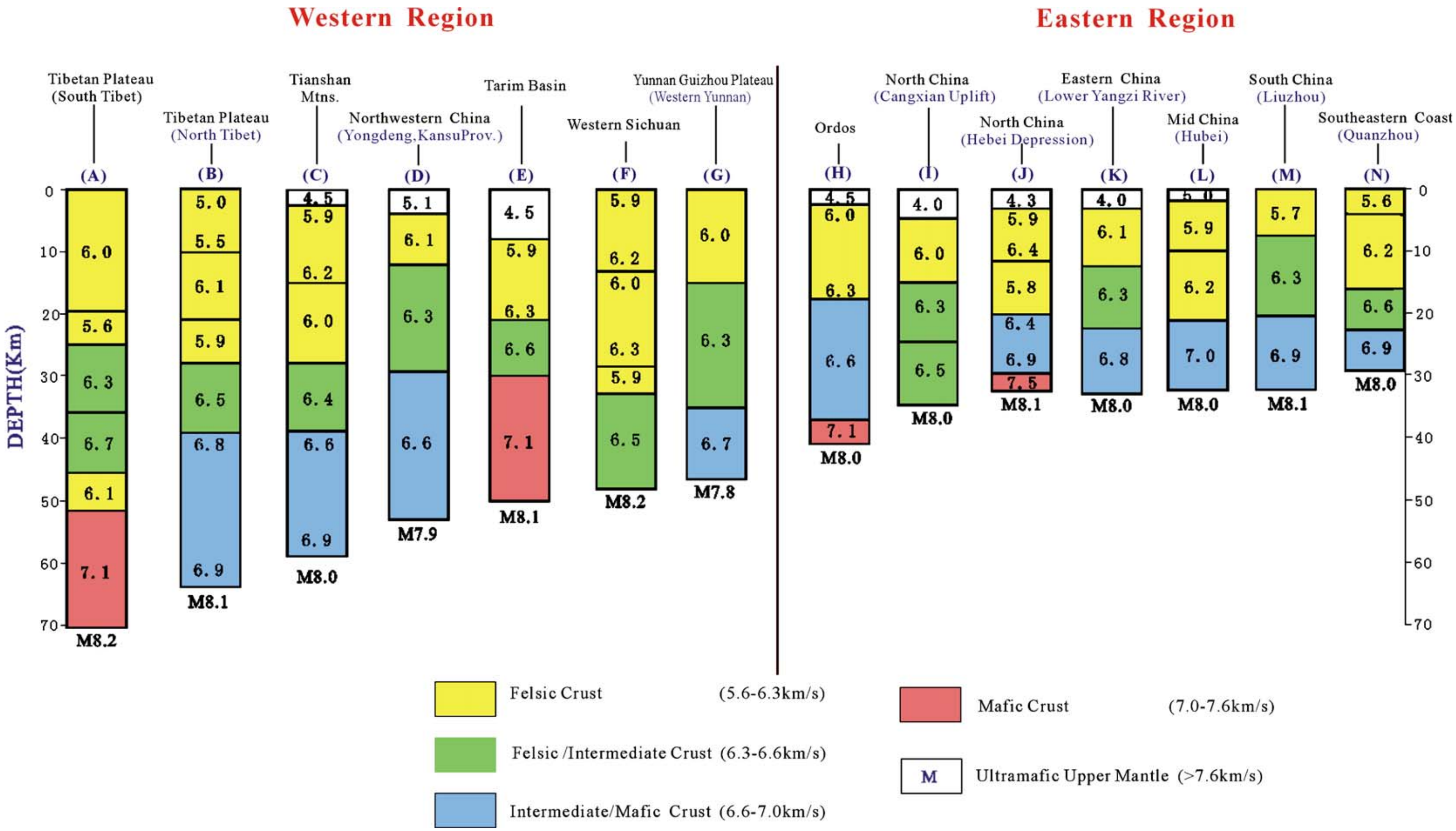

Fig. 5. Representative seismic velocity–depth functions for fourteen regions of China that can be divided into a western region (A–G) and an eastern region (H–N). Letters A–N indicate the position of each column as shown in Fig. 2. Note the low-velocity layer beneath the Tibetan Plateau, Western Sichuan, and Tienshan Mountains that extends to ~25 km depth in the western region. The high-velocity basal crustal layer (≥7.1 km/s) referred to in the text is indicated in red.

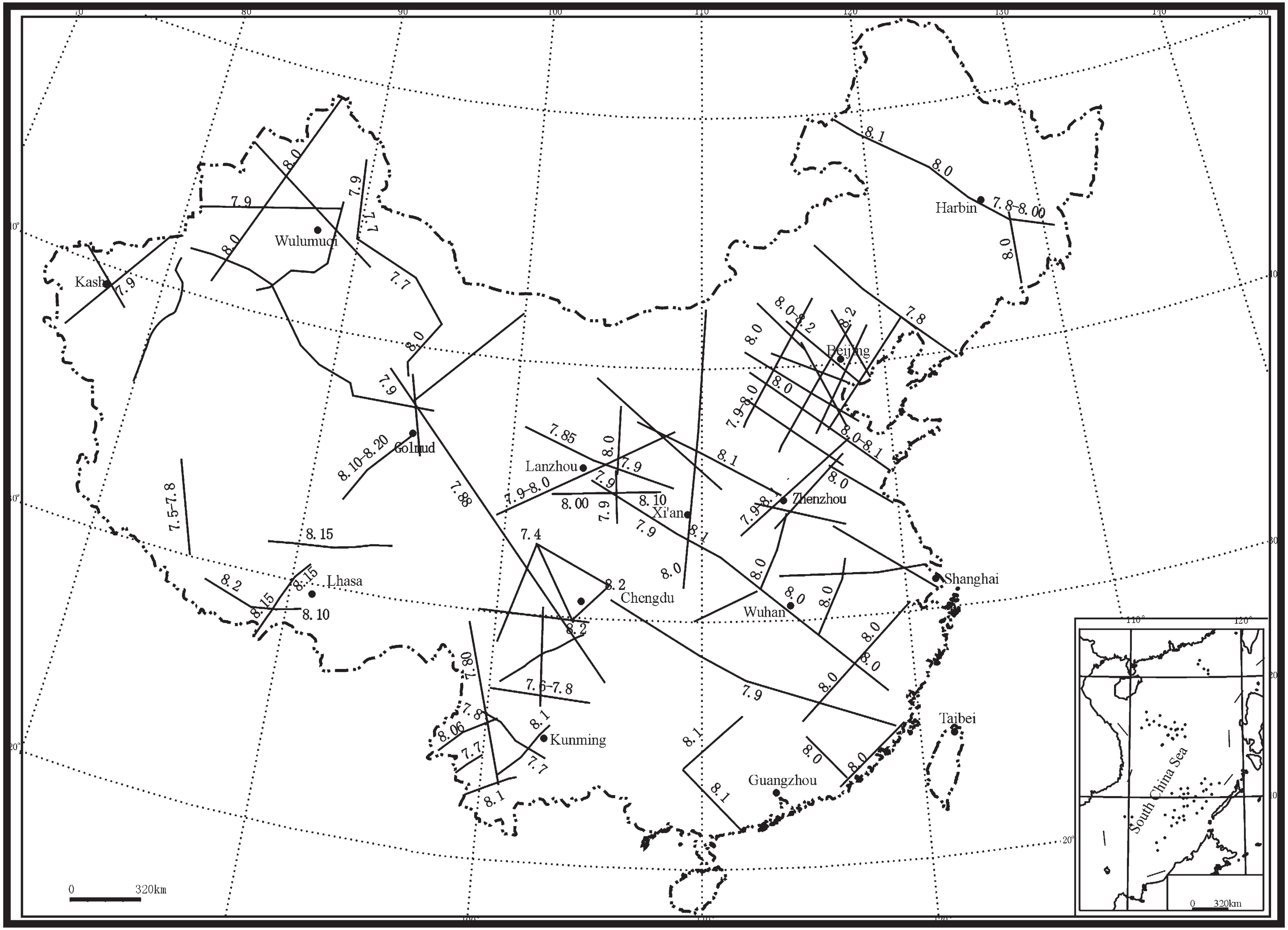

Fig. 6. Seismic velocities of the uppermost mantle from Pn waves. Pn velocities are generally lower in eastern China as compared with those of the Tibetan Plateau.

Another key feature in Fig. 5 is the local presence of low-velocity layers (LVLs) in the crust. The velocity reduction within the LVL is estimated to be 0.3–0.6 km/s (a 5–10% reduction) with respect to the surrounding crust. An LVL usually is found only in orogenic belts, such as in the Tibetan plateau and the Tianshan mountains. In stable regions, this layer is seldom reported. Elsewhere, a crustal low-velocity layer has been reported in the Rhine (Giese et al., 1976) and in the European Alps (Colombi et al., 1973). It has been suggested that the formation of an LVL is related to the high heat flow and abundant felsic rocks in the crust.

Additional evidence for LVLs beneath the Tibetan Plateau and the central Tianshan Mountains has been obtained from receiver function studies (Kind et al., 1996; Nelson et al., 1996; Owens and Zandt, 1997; Kind et al., 2002). To generate an image of crustal structure via receiver functions, waveforms of P and S waves are jointly inverted. INDEPTH studies (Nelson et al., 1996; Kind et al., 1996) have revealed a mid-crustal LVL that is approximately 15–20 km thick. Magnetotelluric data indicates that the middle (15–20 km) and lower (30–40 km) crusts are anomalously conductive (10–30 Ω m) in southern and northern Tibet, respectively (Wei et al., 2001; Unsworth et al., 2004). Basaltic melt is considered to be the preferred explanation for this high conductivity, since aqueous fluids will not connect to form conductive pathways at great depths (>15 km).

Fig. 6 shows seismic velocities of the uppermost mantle from Pn waves. Since Pn waves are often quite weak on DSS profiles, the precision of Pn velocities is limited. However, we observe some consistent patterns in this figure. In general, Pn velocity is quite uniform (7.9–8.0 km/s) and isotropic in the eastern portion of China. In the North–South belt, dividing eastern and western China, the Pn velocity is slightly lower. In the Tibetan Plateau, the Pn velocity is higher for west–east profiles than for north–south profiles. This indicates an anisotropy in the uppermost mantle in the Tibetan Plateau (e.g., Sandvol et al., 1997; Liang et al., 2004). However, for a more robust argument, more profiles from the Tibetan Plateau are needed.

5. Comparisons among DSS profiles, tomographic earthquake studies, and receiver function analyses

There are several tomographic studies (Yi et al., 2000; Eva et al., 2001; Sherburn et al., 2003; Husen et al., 2003; Aktar et al., 2004; Sun et al., 2004a,b; Hearn et al., 2004; Huang and Zhao, 2004; Liang et al., 2004) that show similar patterns of crustal thickness and Pn velocities. We compared our DSS profiles with Sun et al. (2004a,b). While Moho depths vary similarly in both studies, the former provides tighter contours of crustal thickness due to a higher resolution of shot point stations compared to earthquake sources. Moho depth reaches a maximum of 70 km over the Tibetan Plateau in earthquake tomography studies, and 74 km in DSS profiles. Likewise, both DSS and tomography techniques produce a minimum of ~32 km throughout the extended crust of eastern China. The DSS profile's crustal thickness was consistently thicker than the earthquake tomography's crustal thickness in southern China (30°N) by ~5 km, while thinner in northern China (40°N) by ~3 km. The maximum discrepancy, found across the Tibetan plateau (15% of China's area), was 10 km, where DSS profiling yielded a thicker crust.

Several receiver function analyses have generated Moho depths that gradually increase from north to south along the Tibetan Plateau (Zhu and Helmberger, 1998; Kosarev et al., 1999; Vergne et al., 2002; Kind et al., 2002; Tilman et al., 2003; Shi et al., 2004). From NE to SW, the crust thickens from ~50 km beneath the Qaidam basin to ~80 km beneath southern Tibet, where the mean elevation rise is ~2.7 to ~4.8 km above sea level (Vergne et al., 2002). Our DSS profiles reflect the same general trend in the thickening of the crust in those regions from ~54 to ~74 km. Kind et al. (2002) report a decrease in crustal thickness from 78 km in southern Tibet to 65 km in northern Tibet, in good agreement with our contour map (Fig. 4). Meanwhile, Zhu and Helmberger (1998) model a step-like north-to-south increase in crustal thickness along the 95°E meridian, from ~40 km beneath the Qaidam basin to ~55 km approximately 150 km south. These results, both the thickness values and the existence of a step, are inconsistent with the DSS data used to compile our contour map (Fig. 4).

Earthquake tomography studies (Sun et al., 2004a,b) have also revealed that Pn velocities tend to be higher than 8.0 km/s in western China and less than or equal to 8.0 km/s in eastern China. These observations are generally consistent with Pn velocities measured by DSS profiling. Pn velocities are between 7.9 and 8.2 km/s beneath the Tibetan plateau, whereas Pn velocities generally do not exceed 8.0 km/s beneath eastern China (Fig. 5). However, the pattern is less clear due to inaccuracies caused by the shortness of path lengths between shot point stations, the dependency of the Pn velocity for a directed seismic wave on the grain of the rock, and relatively few ray paths compared to earthquake databases. The Tianshan and Junngar basins show Pn velocities less than or equal to 8.0 km/s in both DSS and most seismic tomography studies.

It appears that, for presently available data in China, DSS profiling is a more accurate method for determining Moho depth, due to the high density of shot points and recording stations, whereas earthquake tomography yields more reliable estimates of Pn velocities due to the large number of travel-time paths that can be averaged for a more robust calculation.

6. Conclusions

1) There is a north–south-trending belt at 103–105° east longitude with a strong lateral gradient in crustal thickness. This belt is coincident with the north–south seismic belt and the north–south gravity anomaly belt. It divides China into an eastern portion, with a crustal thickness of 30–46 km, and a western portion, with a thickness of 46–74 km.
2) The topography of the Tibetan plateau is rather flat, whereas the crustal thickness decreases from 74 km in the south to 52 km in the northeast. The Tibetan plateau also has remarkably steep gradients in crustal thickness along its margins.
3) In western China, the isolines of the crustal thickness show an east–west trend, while in eastern China they are in NNE direction. These patterns reflect the fact that the crusts of eastern and western China are in two different stress fields and have experienced different evolutionary processes. The crust of the western portion is strongly compressed in the NS direction and becomes thicker, while the crust of the eastern portion has thinned by being stretched in the NS direction.
4) There is a close relationship between crustal thickness and tectonic setting. In depressions and basins, the crust is thinner than that in adjacent regions, while in uplifted regions, the crust is thicker than in surrounding regions.
5) In some stable regions such as the Tarim basin and Ordos plateau, there is a high-velocity (7.1 km/s) layer in the lower crust. However, in much of eastern China and young orogenic belts, such a layer is absent. One exception is southern Tibet, where the high-velocity layer is related to the northward injection of the cold Indian Plate. Beneath northern Tibet, there appears to be no such layer. The missing high-velocity layer may be due to the widespread delamination of the lower crust and sub-crustal lithosphere during both extensional (eastern China) and compressional (Tianshan and northern Tibet) orogenies. Such widespread delamination has important implications for estimating the bulk composition of the continental crust.
6) In orogenic belts, there is a low-velocity layer (LVL) in the middle crust where the P-wave velocity decreases by 5–10%. The LVL is also imaged in receiver functions and geoelectrical studies (where it is manifest as a high conductivity zone). In stable regions this layer seldom exists. It seems that the formation of the LVL is related to the high mid-crustal temperature and the abundant felsic rock in the crust.
7) DSS profiles provide the best resolution of crustal thickness, while earthquake tomography techniques yield more reliable Pn velocities. Crustal thicknesses derived from these two techniques tend to agree within ±3–5 km.

Acknowledgements

This work was supported by the National Natural Science Foundation of China (Grant No. 40374032), the Ministry of Science and Technology of China (Grant No. 95-13-02-02), and the U. S. Geological Survey. We are also grateful to Ms. Hongzhao Deng for her figure plotting. Reviews by G. R. Keller and B. Yang were constructive and helpful. Additional suggestions from G. Chulick, R. Mereu, J. Mechie, S.T. McDonald, and S. Detweiler greatly improved the text.

References

Aktar, M., Dorbath, C., Arpat, E., 2004. The seismic velocity and fault structure of the Erzincan Basin, Turkey, using local earthquake tomography. Geophys. J. Int. 156 (3), 497–505.

Christensen, N.I., Mooney, W.D., 1995. Seismic velocity structure and composition of the continental crust: a global view. J. Geophys. Res. 100 (B7), 9761–9788.

Colombi, B., et al., 1973. Preliminary report on the seismic refraction profile Gargano–Salemo–Palermo–Pantelleria. Boll. Geofis. Teor. Appl. 15, 59.

Dewey, J.F., Cande, S., Pitman, W.C., 1989. Tectonic evolution of the India–Eurasia collision zone. Eclogae Geol. Helv. 82, 717–734.

Ding, G.Y., 1991. Relative motions of sub-plates and active blocks. Introduction to Lithospheric Dynamics of China. Seismological Press, Beijing, pp. 142–153.

Eva, E., Solarino, S., Spallarossa, D., 2001. Seismicity and crustal structure beneath the western Ligurian Sea derived from local earthquake tomography. Tectonophysics 339 (3–4), 495–510.

Filatova, N.I., 2004. Cenozoic extension structures in the continental framework of the Japan Sea. Geotectonics 38, 459–477.

Gao, S., Zhang, B.R., Jin, Z.M., Kern, H., Luo, T.C., Zhao, Z.D., 1998. How mafic is the lower continental crust? Earth Planet. Sci. Lett. 161, 101–117.

Giese, P., Prodehl, C., Stein, A., 1976. Explosion Seismology in Central Europe. Springer-Verlag, New York. 429 pp.

Hearn, T.M., Wang, S., Ni, J.F., Xu, Z., Yu, Y., Zhang, X., 2004. Uppermost mantle velocities beneath China and surrounding areas. J. Geophys. Res. 109, doi:10.1029/2003JB002874. 11 pp.

Hsu, K.J., Li, J.L., Chen, H.H., Wang, Q.C., Sun, S., Sengor, A.M.C., 1990. Tectonics of South China: key to understanding West Pacific geology. Tectonophysics 183, 9–39.

Huang, J., Zhao, D., 2004. Crustal heterogeneity and seismotectonics of the region around Beijing, China. Tectonophysics 385 (1–4), 159–180.

Huang, T.K., Jen, C., Jiang, C., Chang, Z., Chin, D., 1980. The Geotectonic Evolution of China. Academic Publishing House, Beijing, China. 124 pp.

Husen, S., Quintero, R., Kissling, E., Hacker, B., 2003. Subduction-zone structure and magmatic processes beneath Costa Rica constrained by local earthquake tomography and petrological modelling. Geophys. J. Int. 155 (1), 11–32.

Kind, R., Ni, J., Zhao, W., Wu, J., Yuan, X., Zhao, L., Sandvol, E., Reese, C., Nabelek, J., Hearn, T., 1996. Evidence from earthquake data for a partially molten crustal layer in southern Tibet. Science 274, 1692–1694.

Kind, R., Yuan, X., Saul, J., Nelson, D., Sobolev, S.V., Mechie, J., Zhao, W., Kosarev, G., Ni, J., Achauer, U., Jiang, M., 2002. Seismic images of the crust and upper mantle beneath Tibet: evidence for Eurasian plate subduction. Science 298, 1219–1221.

Kosarev, G., Kind, R., Sobolev, S.V., Yuan, X., Hanka, W., Oreshin, S., 1999. Seismic evidence for a detached Indian lithospheric mantle beneath Tibet. Science 283, 1306–1309.

Liang, C., Song, X., Huang, J.L., 2004. Tomographic inversion of Pn travel times in China. J Geophys. Res. 109, doi:10.1029/2003JB002789. 19 pp.

Li, S.L., Mooney, W.D., 1998. Crustal structure of China from deep seismic sounding profiles. Tectonophysics 288, 105–113.

Liu, M., Cui, X., Liu, F., 2004. Cenozoic rifting and volcanism in eastern China; a mantle dynamic link to the Indo-Asian collision?; asthenosphere–lithosphere dynamic responses to Tethyan plate collisions. Tectonophysics 393, 29–42.

Ma, X.Y., 1989. Atlas of Lithospheric Dynamics of China. China Cartographic Publishing House, Beijing, China. 70 pp.

Meng, Q., Wang, E., Hu, J., 2005. Mesozoic sedimentary evolution of the northwest Sichuan basin; implication for continued clockwise rotation of the South China block. Geol. Soc. Amer. Bull. 117, 396–410.

Molnar, P., England, P., Martinod, J., 1993. Mantle dynamics, the uplift of the Tibetan Plateau and the Indian monsoon. Rev. Geophys. 31, 357–396.

Mooney, W.D., 1989. Seismic methods for determining earthquake source parameters and lithospheric structure. In: Pakiser, L.C., Mooney, W.D. (Eds.), Geophysical Framework of the Continental United States. Geol. Soc. Am. Mem., vol. 172, pp. 11–34.

Mooney, W.D., Prodehl, C., Pavlenkova, N.I., 2002. Seismic velocity structure of the continental lithosphere from controlled source data. International Handbook of Earthquake and Engineering Seismology, vol. 81A, pp. 887–910.

Nelson, K.D., et al., 1996. Partially molten middle crust beneath southern Tibet: synthesis of project INDEPTH results. Science 274, 1684–1688.

Owens, T.J., Zandt, G., 1997. Implications of crustal property variations for models of Tibetan plateau evolution. Nature 387, 37–43.

Patriat, P., Achache, J., 1984. India–Eurasia collision chronology has implications for crustal shortening and driving mechanism of plates. Nature 311, 615–621.

Research Center of Exploration Geophysics, China Earthquake Administration, 2004. Notes on Earthquake Monitoring and Prediction of RCEG. Seismological Press, Beijing, pp. 20–21 (in Chinese).

Sandvol, E., Ni, J., Kind, R., Zhao, W.J., 1997. Seismic anisotropy beneath the southern Himalayas–Tibet collision zone. J. Geophys. Res. 102, 17,813–17,823.

Sherburn, S., Bannister, S., Bibby, H., 2003. Seismic velocity structure of the central Taupo volcanic zone, New Zealand, from local earthquake tomography. J. Volcanol. Geotherm. Res. 122 (1–2), 69–88.

Shi, D., Zhao, W.J., Brown, L., Nelson, D., Zhao, X., Kind, R., Ni, J., Xiong, J., Mechie, J., Guo, J., Klemperer, S., Hearn, T., 2004. Detection of southward intracontinental subduction of Tibetan lithosphere along the Bangong–Nujiang suture by P-to-S converted waves. Geology 32, 209–212.

Sun, Y.S., Morgan, D., Toksov, M.N., 2004a. 3D P- and S-velocity models for the crust and uppermost mantle of China by Monte-Carlo adaptive moving window inversion. Seismol. Res. Lett. 74, 202–203.

Sun, Y.S., Li, X., Kuleli, S., Morgan, F.D., Toksov, M.N., 2004b. Adaptive moving window method for 3D P-velocity tomography and its application in China. Bull. Seismol. Soc. Am. 94, 740–746.

Tilman, F., Ni, J., the INDEPTH III Seismic Team, 2003. Seismic imaging of the downgoing Indian lithosphere beneath central Tibet. Science 300, 1424–1427.

Unsworth, M., Wei, W., Jones, A., Shenghiu, L., Bedrosian, P., Booker, J., Jin, S., Deng, M., Tan, H., 2004. Crustal and upper mantle structure of northern Tibet imaged with magnetotelluric data. J. Geophys. Res. 109, doi:10.1029/2002JB002305.

Vergne, J., Wittlinger, G., Hui, Q., Tapponnier, P., Poupinet, G., Mei, J., Herquel, G., Paul, A., 2002. Seismic evidence for stepwise thickening of the crust across the NE Tibetan plateau. Earth Planet. Sci. Lett. 203, 25–33.

Wei, W., Unsworth, M., Jones, A., Booker, J., Tan, H., Nelson, D., Chen, L., Li, S., Solon, K., Bedrosian, P., Jin, S., Deng, M., Ledo, J., Kay, D., Roberts, B., 2001. Detection of widespread fluids in the Tibetan crust by magnetotelluric studies. Science 292, 716–718.

Yi, X., Futian, L., Jianhua, L., Ruomei, S., 2000. Crustal structure and tectonic setting of the Tien Shan seismic zone, Xinjiang, China. Acta Geophys. Sin. 43 (2), 184–193.

Yuan, Xuecheng, 1996. Atlas of Geophysics in China. Geological Publishing House, Beijing. 217 pp.

Zelt, C.A., Smith, R.B., 1992. Seismic travel time inversion for 2-D crustal velocity structure. Geophys. J. Int. 108, 16–34.

Zhao, W.L., Morgan, W.J., 1987. Injection of Indian crust into Tibetan lower crust: a two-dimensional finite element model study. Tectonics 6, 489–504.

Zhao, Z.Y., Windley, B.F., 1990. Cenozoic tectonic extension and inversion of the Jizhong Basin, Hebei, North China. Tectonophysics 185, 83–89.

Zhao, W., Nelson, K.D., the Project INDEPTH Team, 1993. Deep seismic reflection evidence for continental underthrusting beneath southern Tibet. Nature 366, 557–559.

Zhu, L., Helmberger, D.V., 1998. Moho offset across the northern margin of the Tibetan Plateau. Science 281, 1170–1172.